# The Nevada Winter Storm of 14-16 April 2009

Ryan Knutsvig and Clair Ketchum
NOAA/National Weather Service Forecast Office Elko, Nevada

## 1. Introduction

An unseasonably strong late season winter storm impacted northern and central NV on 14-16 April 2009. This major storm brought heavy snow accumulations (Fig. 1), strong winds, and blowing and drifting snow to much of northern NV. For the period of 15-16 April, Eureka, NV, storm total snowfall was 26 inches. This ranked as Eureka's second highest two-day snowfall accumulation ever recorded. Further north in Lamoille, NV, the two-day snowfall total of 21 inches ranked as the all-time highest.

As mentioned, heavy snow combined with strong winds during this event. Spotters living in Austin and Eureka reported snow drifts over three feet high. National Weather Service (NWS) personnel also reported two to three feet of snow accumulation in the Eureka area with higher drifts (Fig. 2). Due to the impact of this storm, the main motivation for this paper will be to aid operational forecasters in the diagnoses of future, similar winter storms impacting northern NV.

## 2. Data and Methodology

All model data was archived at the NWS Weather Forecast Office (WFO) in Elko, NV. The Weather Event Simulator (WES) was used to view the data. Snowfall data were collected using NWS trained cooperative observers, as well as the Snowpack Telemetry (SNOTEL) observation sites that are managed and funded by the National Resources Conservation Service (NRCS). Rainfall/snow-water equivalent measurements were taken from Automated Surface Observing System (ASOS) and Automated Weather Observing System (AWOS) observations from local airports in the County Warning Area (CWA). Standardized climatological anomalies were computed using data from a 30-year climatology (1971-2000) and the NCEP-NCAR global reanalysis data (Graham and Grumm, 2010).

**3. Synoptic Overview**

The upper level pattern leading up to the 14-16 April storm included a broad trough over the Gulf of AK, an upper low slowly exiting the Desert Southwest, and weak ridging over the western United States. This Gulf of AK trough then drifted east and closed off over Vancouver Island, BC by 0000 UTC on 14 April. An upper jet located southeast of this upper low was depicted by the GFS analysis at 1200 UTC. This jet had a maximum wind speed of 51 m $s^{-1}$ (99 knots) at 300 hPa and extended from northern CA to western MT. The upper low moved southward across the Pacific Northwest and into northeastern CA/northwestern NV by 0000 UTC15 April (Fig. 3).The system's 500 hPa geopotential heights were at a minimum at this time, being around 5400 meters before drifting southeast into south-central NV. The low then slowly exited eastward and was centered over south-central UT by 1200 UTC on 16 April.

At the surface, a stationary surface frontal boundary extended from central ID southwest into northern CA at 0000 UTC 14 April. The boundary had shifted southeastward by 1200 UTC as a cold front and extended southwestward from eastern ID through central NV and into southeastern CA (Fig.4). By 0000 UTC 15 April, the surface low had decreased to 992 hPa but was nearly stationary, continuing to remain in central

NV (Fig. 5). The surface low then drifted off into west-central UT by 0600 UTC 15 April. By 1800 UTC on 15 April, the surface low was centered over eastern-central UT before drifting into the central Rockies for most of 16 April.

**4. Anomalies**

The standardized anomalies, as described in Graham and Grumm (2010), were the most significant at 250 hPa and at the surface. Table 1 indicates that the 250 hPa temperature anomalies (Fig. 6) and the surface mean sea-level pressure (MSLP) anomalies (Fig. 7) valid at 0000 UTC on 15 April were the most significant being three to four standard deviations (SD) above and below average, respectively. The strong warming at 250 hPa is indicative of a strong tropopause fold, as described in Hirschberg and Fritsch (1991). The return periods for both of the variables are around one month in the western U.S. Also, the standardized geopotential height anomaly at 500 hPa was two to three SD below normal (Fig 8).

**5. Tropopause Fold**

As discussed above, this event exhibited a significant tropopause fold. Research in the area of tropopause folds has been mainly centered upon winter storms over the Midwest and East Coast. A major study completed by Uccellini, et al (1985) focused on the very strong President's Day Cyclone of 18-19 February 1979. It was noted that 12 to 24 hours prior to the event, an upper level trough and associated strong tropopause fold progressed east across the mid-central U.S. During this event, the tropopause fold was identified west of the winter storm, and during the ensuing interaction between the tropopause fold and surface cyclone, rapid and deep cyclogenesis occurred, which resulted in a major winter storm. It was summarized in the paper that the injection of stratospheric air into the low levels of the troposphere brought about a significant increase in absolute vorticity due to "adiabatic mass convergence, vertical stretching, and the related decrease in the static stability of the air mass originating in the stratosphere."

In the storm discussed in this paper, a tropopause fold was evident off the coast of northwest CA on the PV1.5 surface at 1200 UTC on 14 April (Fig. 9). Meanwhile, an area of low pressure at the surface was stationed near south-central Nevada with a central pressure of 1002 hPa. Interestingly, the distance between the two features was roughly 500 nautical miles. By 1800 UTC on 14 April, the tropopause fold lowered to a depth of 707 hPa over central CA, while the surface pressure of the low deepened to 997 hPa and maintained its position across south-central NV, per the GFS analysis. The surface low continued its deepening through 0000 UTC on 15 April, while the tropopause fold moved across southern CA (Fig. 10). The interaction between the tropopause fold and the developing surface low is similar to what has been documented during the President's Day storm of 1979. It is clear that strong lee-side cyclogenesis was underway across NV at this time as the MSLP analyses for 1200 UTC 14 April and 0000 UTC 15 April (Figs. 4 and 5 respectively) depict a significant drop in surface pressure of 13 hPa in 12 hours.

**6. Frontogenesis**

Frontogenesis increased across NV by 0000 UTC on 15 April in association with the cold front. The strongest frontogenesis occurred from the surface up through 500 hPa according to the 20-km RUC analysis (Figs. 11 and 12). The RUC analyses were used because of the higher temporal resolution compared to the 40-km GFS. The RUC showed frontogenesis increasing between 2000 UTC and 2300 UTC 14 April, diminishing overnight through 1200 UTC. Also evident in the analyses was the existence of negative saturated equivalent potential vorticity (EPV*) above the frontogenesis. The negative EPV aloft suggests there is Conditional Symmetric Instability (CSI) present, which is an environment that favors slantwise convection. When strong linear forcing is present in this environment, e.g. frontogenesis, heavy banded precipitation can form. Initially, it was thought that banded convection occurred around 2000 UTC in north-central NV (Fig. 13). However, from tracking the origin of the reflectivity and verifying with satellite imagery, it was determined that the bands were the result of chaff being released from military aircraft. Authentic banding did occur overnight in the Eureka, NV area, however. This banding is evident at the southeastern edge of the KLRX radar coverage area at 1000 UTC 15 April (Fig. 14).

One aspect the authors chose to examine was the depth of the dendritic growth zone (DGZ) and the relationship to strong upward vertical velocities. The depth of the DGZ was over one km in the vicinity of the frontal boundary. It is believed that the co-location of a thick DGZ and strong frontogenetical forcing led to enhanced snowfall across the area. Frontal broadening of the DGZ can be expected with most cold fronts. As the lower part of the front approaches, the isotherms closer to the ground (-12C) descend toward the surface, while the upper part (-18C) remains unchanged. Hence, the -12 to -18C layer becomes deeper with the approach of the front. Theoretically, a strong front with less vertical slope (the surface front well out ahead of the mid-level front) would have a deeper DGZ. However, the deeper the DGZ, the more stable the profile would be.

Essentially, conditions that favor a high dendritic snow growth rate include high values of omega in a deep DGZ. The use of omega and temperatures to diagnose when the best snow production will occur was described in Cobb and Waldstreicher (2005). Four panel images of the DGZ depth, frontogenesis in the -18 to -12 C layer, omega in the -18 to -12 C layer, and relative humidity in the -18 to -12 C layer from the RUC analyses (Figs. 15-17) show that there was a large area of deep DGZ depth in close proximity to the frontogenesis. The DGZ depth was over 1.3 km and was as high as 1.8 km according to the RUC. This was combined with frontogenesis between 200 and 500 units (K/m/1e10s) within that same layer (-18 to -12C layer). Frontogenesis decreased quickly after 1200 UTC 15 April.

Most of the precipitation associated with the frontogenesis fell during the early morning hours of the 15$^{th}$. According to precipitation totals from the Eureka COOP observer valid on the 15$^{th}$ of April, Eureka received 16 inches of snow with 1.25” of water equivalent. The airport (KP68) is eight nautical miles NNE of the city of Eureka and received 0.73” of water equivalent precipitation.

**7. Prolonged Isentropic Lift**

The second significant period of snowfall for Eureka occurred on the night of 15 April. As the upper low pushed east across central NV and into UT, “wrap-around precipitation” began as a plume of moisture wrapped northwestward around the low pressure system. Examining pressure and wind on the 295 K isentropic surface from the RUC analyses (Fig. 18) reveals that strong isentropic lift occurred on the night of the 15$^{th}$ (0500 to 1100 UTC 16 April).

A weak trough of warm air aloft (trowal) also is evident in the model analyses, particularly on 16 April (Fig. 19). As noted in Martin (1998), precipitation on the back side of a low pressure system often occurs in the vicinity of the trowal. This ridge of higher equivalent potential temperature signifies a higher moisture/temperature air stream that ascends as it gets "wrapped around" the back side of a low pressure system. Often frontogenesis is co-located with this air stream that is a maximum of saturated equivalent potential temperature.

## 8. Orographic Enhancement of Snow

Vertical motion influence by terrain played a significant role in the spatial distribution of snowfall in this event. The cold front moved southeast across NV from the afternoon on the 14$^{th}$ through the early morning hours of the 15$^{th}$. During this time, strong southeasterly isentropic lift was occurring aloft as warm air was pushing northward ahead of the main upper level low. Thus, a broad area of upward motion was occurring during and after the cold frontal passage. As the snow descended into the lowest one km of the atmosphere, it encountered either enhanced snow growth in the upslope regions of the terrain or inhibited snow growth and sublimation in the downslope regions of the terrain. Figure 20 shows the NAM12 sounding for the Eureka, NV airport (KP68) valid 1200 UTC 15 April. A close examination of the sounding and the local terrain reveals that the inversion base is around 0.5 km above the peaks of the mountain ranges. The close proximity of the inversion to the mountain barriers likely led to strong mountain wave action, which led to a significant snowfall increase in the upslope regions and decrease in the downslope regions. The cold frontal inversion was in place until around 1800 UTC on the 15th. From 1800 UTC on the 15th through the morning of the 16th, the profile was nearly moist adiabatic from the surface to around 450 hPa with northerly flow throughout the entire profile.

The most significant contributor to the enhanced snowfall at Eureka and Lamoille, NV, was the prolonged period of upslope snow enhancement. Eureka, NV lies at the intersection of the Diamond Mountains and the Fish Creek Range. The terrain favors enhanced convergence and upslope in north-northwesterly flow as Eureka lies in a “horseshoe” or u-shaped valley with mountains to the east, south, and west. The Moderate Resolution Imaging Spectroradiometer (MODIS) imagery reveals that, one day after the event, the snowfall had melted considerably in the April sun and was significantly limited to the north-facing slopes and higher terrain (Fig. 21). A closer look at the MODIS imagery (Fig. 22) shows that indeed the northwest facing slopes received the most snowfall. This was confirmed by observations from Elko, NV (non-upslope area - 8.3”) and Spring Creek and Lamoille, NV (upslope areas – 23” and 21”, respectively).

## 9. Observations and Summary

The winter storm of April 15-16th 2009 resulted in the highest two-day snowfall total recorded for Lamoille, NV and the second for Eureka, NV. Impacts included power outages in the Eureka, NV area, and 23 motor vehicle accidents reported by the Nevada Highway Patrol.

The significant meteorological features that accompanied this event include:

1. Strong upper level temperature and MSLP anomalies (return intervals of 1 per month)
2. Strong tropopause fold (PV1.5 surface extended down to near 700 hPa)
3. Rapid surface cyclogenesis
4. Strong frontogenesis combined with negative EPV* aloft and a deep DGZ
5. Prolonged mid-level isentropic lift ahead of the low and later in the event associated with the trowal
6. Prolonged period of upslope enhancement for north facing slopes

## 10. Acknowledgements

The authors wish to thank Randy Graham, Science and Operations Officer, NWS Salt Lake City and Richard Grumm, Science and Operations Officer, NWS State College for their assistance in providing the climatological anomaly maps for this storm. A special thank you goes to David Myrick, Science and Operations Officer, NWS Reno for assisting the authors in gathering journal articles for this case. And finally, the authors thank Chris Smallcomb, Deputy Chief of Western Region - Scientific Services Division for proofreading this document.

## 11. References

Cobb, D. K, and J. S. Waldstreicher, 2005: A simple physically based snowfall algorithm. The 21st Conference on Weather Analysis and Forecasting/17th Conference on Numerical Weather Prediction (Washington, DC), 28 Jul-5 Aug, 2005.

Graham, Randall A., and Richard H. Grumm, 2010: Utilizing Normalized Anomalies to Assess Synoptic-Scale Weather Events in the Western United States. *Wea. Forecasting*, **25**, 428-445.

Hirschberg, P.A., and J.M. Fritsch, 1991: Tropopause Undulations and the Development Of Extratropical Cyclones. Part 2: Diagnostic Analysis and Conceptual Model. *Mon. Wea. Rev.*, **119**, 518-550.

Uccellini, L. W., D. Keyser, K. F. Brill and C. H. Wash, 1985: The Presidents' Day Cyclone of 18-19 February 1979: Influence of Upstream Trough Amplification and Associated Tropopause Folding on Rapid Cyclogenesis. *Mon. Wea. Rev*., **113**, 962-988.

Martin, J. E., 1998: The Structure and Evolution of a Continental Winter Cyclone. Part II: Frontal Forcing of an Extreme Snow Event. *Mon. Wea. Rev*., **126**, 329-348.

# TABLES AND FIGURES

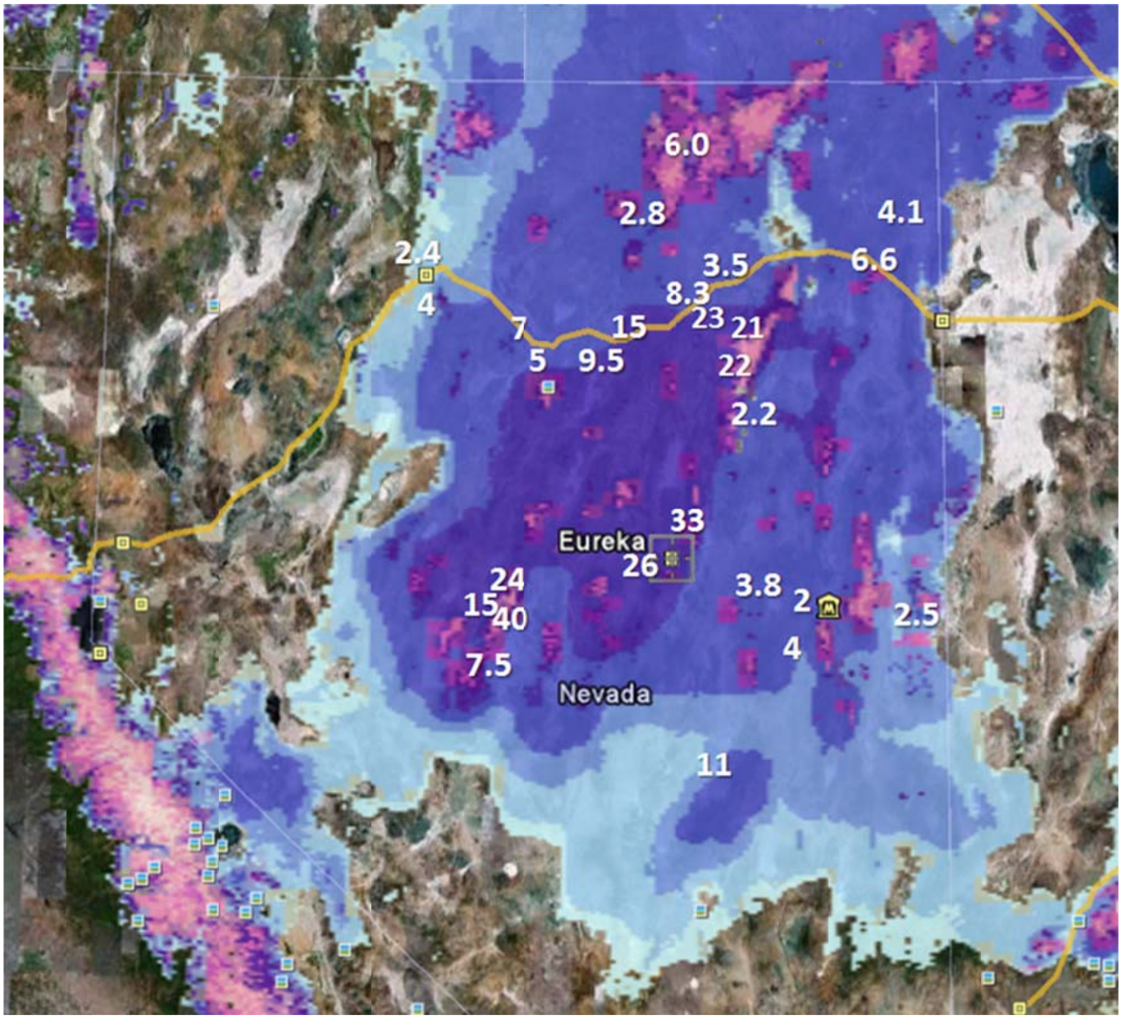
6.0
2.8
4.1
2.4
3.5
6.6
8.3
4
7
15
23
21
5
9.5
22
2.2
33
Eureka
26
3.8
2
2.5
24
15
40
4
7.5
Nevada
11

**inches,**

**Figure 2: Picture of the storm snow accumulation in Eureka, NV on April 16, 2009. Photo courtesy Eureka County Emergency Manager Ron Damahle.**

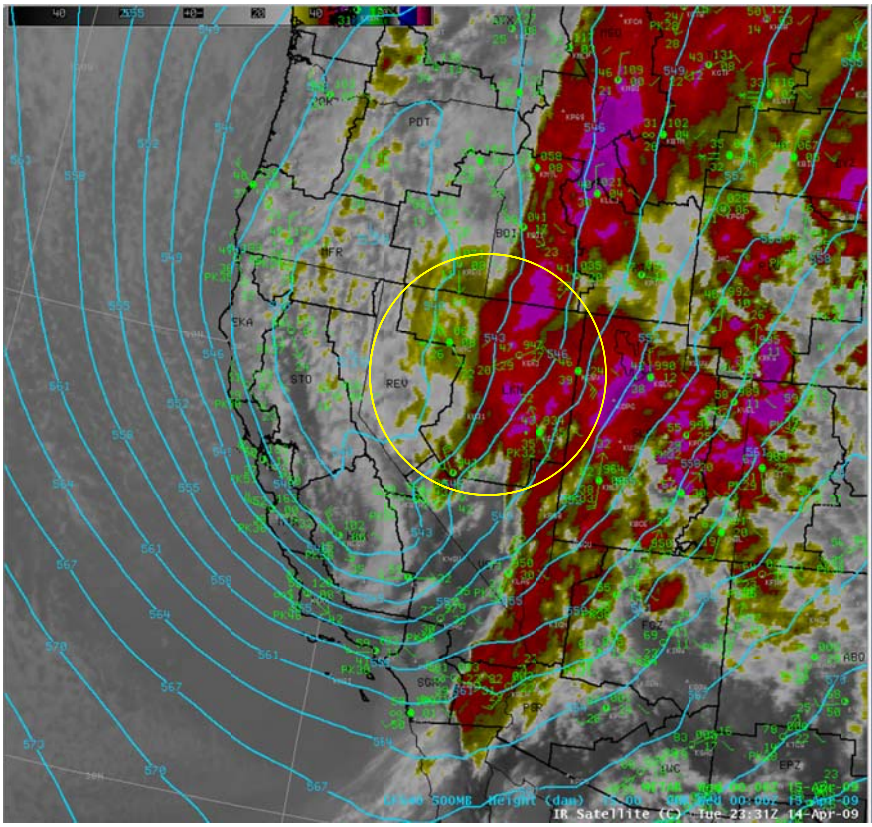

**Figure 3: Infrared satellite imagery at 2331 UTC 14 April 2009 with GFS 500 hPa geopotential height analysis (aqua, solid, in dm) and surface observations (green) overlaid and valid at 0000 UTC 15 April 2009. Elko's CWA is circled in yellow.**

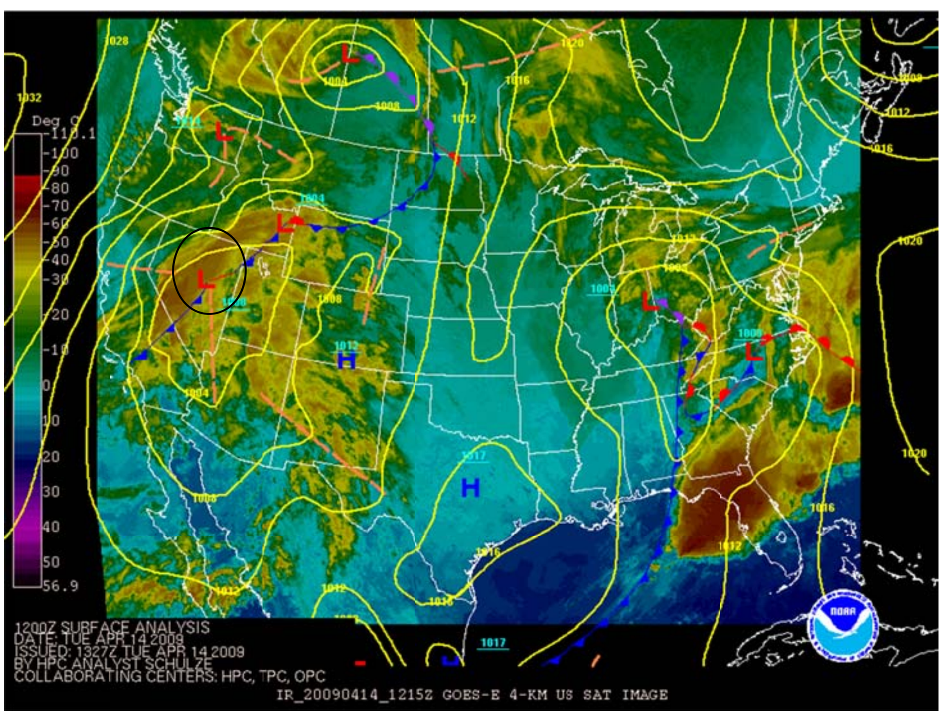


**Figure 4: IR satellite imagery and surface analysis valid at 1200 UTC on 14 April 2009. Isobars (yellow) are in hPa. Elko's CWA is circled in black.**

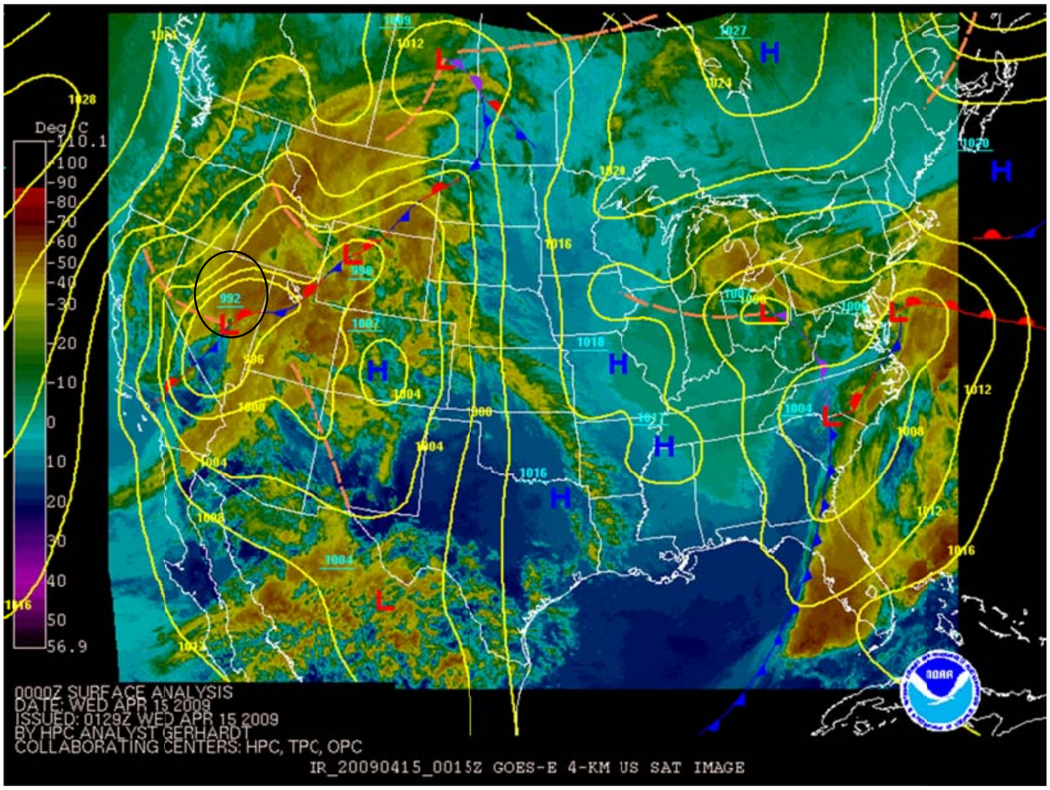


**Figure 5: As in Figure 4 except valid at 0000 UTC on 15 April 2009.**

| Variable | Standard Deviations | Return Period |
|---|---|---|
| 250 hPa Temperature | 3 to 4 | About 1 per month |
| 500 hPa Heights | -2 to -3 | > 1 per month |
| Surface MSLP | -3 to -4 | About 1 per month |

**Table 1: Return intervals for standardized anomalies.**

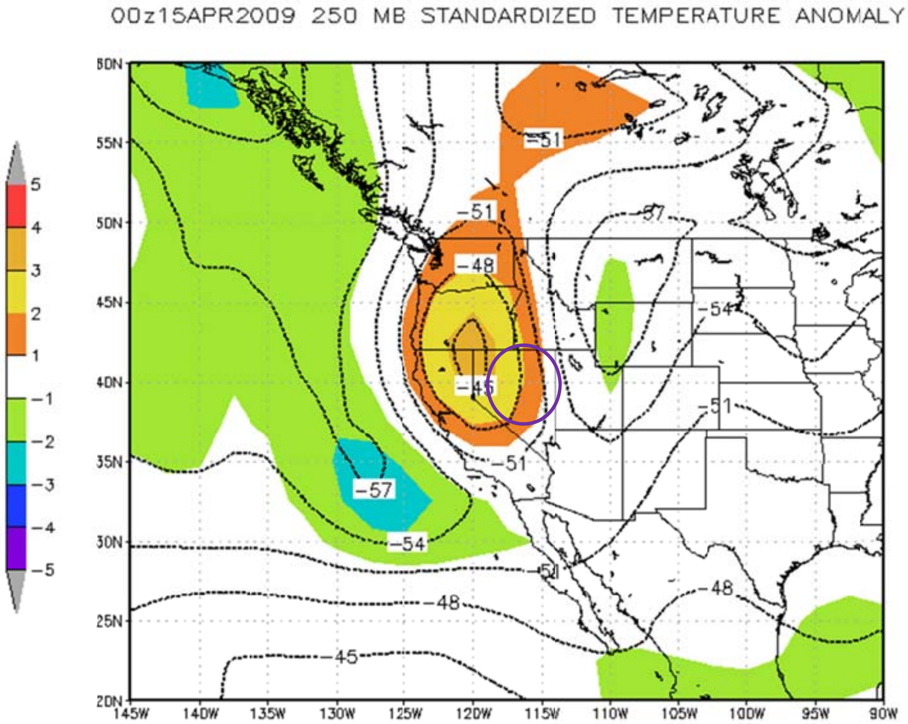


**Figure 6: NCEP GFS 00-hour forecasts showing 250 hPa temperature and temperature anomalies from 0000 UTC 15 Apr 2009.Temperatures every 3C, anomalies in standard deviations from normal. Elko's CWA is circled in magenta.**

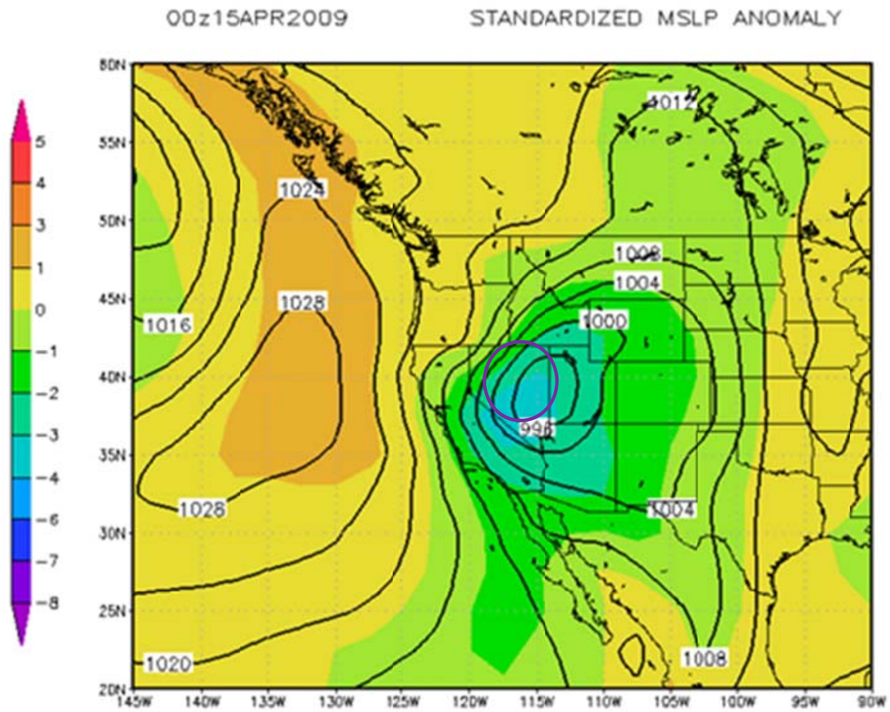


**Figure 7: As in figure 5 except for mean sea level pressure, in hPa, and mean sea level pressure anomalies.**

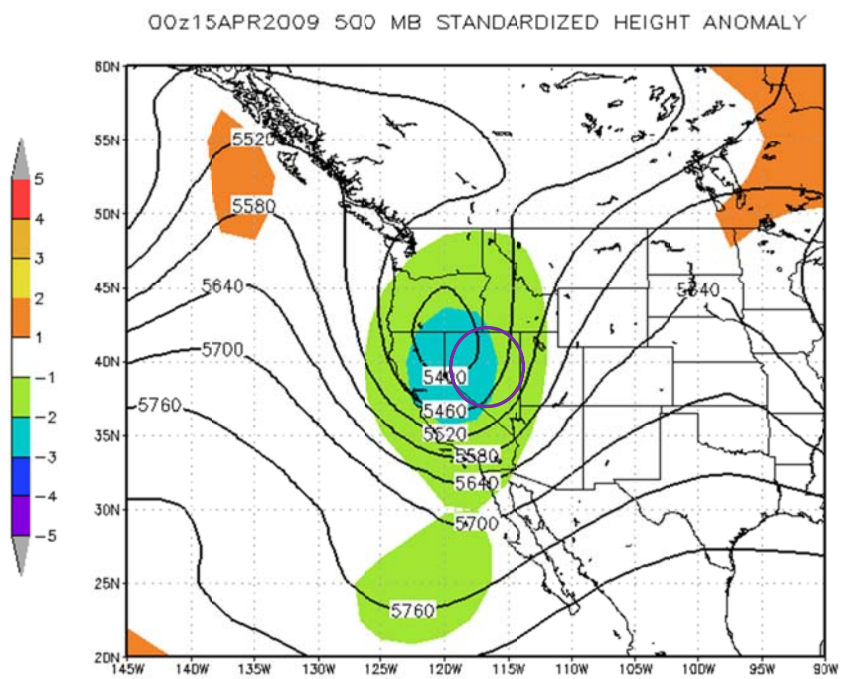


**Figure 8: As in Figure 5 except for 500 hPa height, in meters, and height anomalies.**

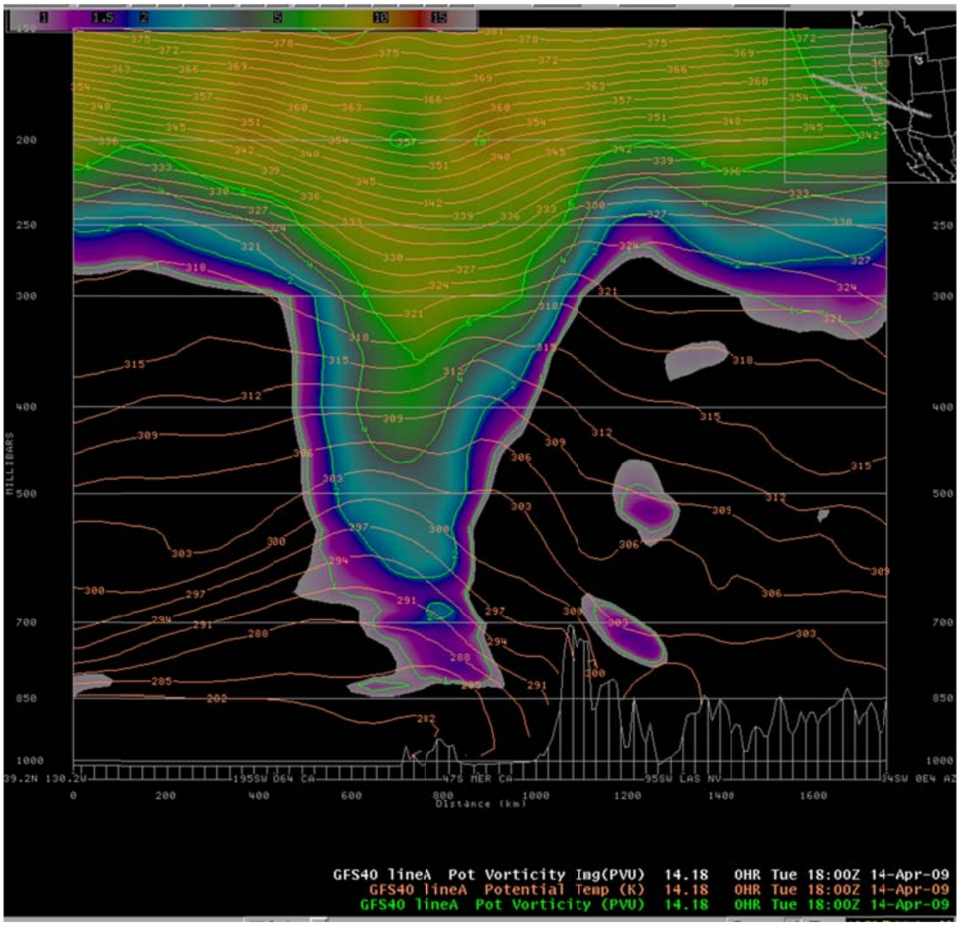


**Figure 9: GFS40 00-hour forecast at 1800 UTC 14 April 2009 depicting cross section of the potential vorticity (PV) (image) with potential temperature (orange lines, solid, in K). The PV 1.5 surface extends down to near 700 hPa.**

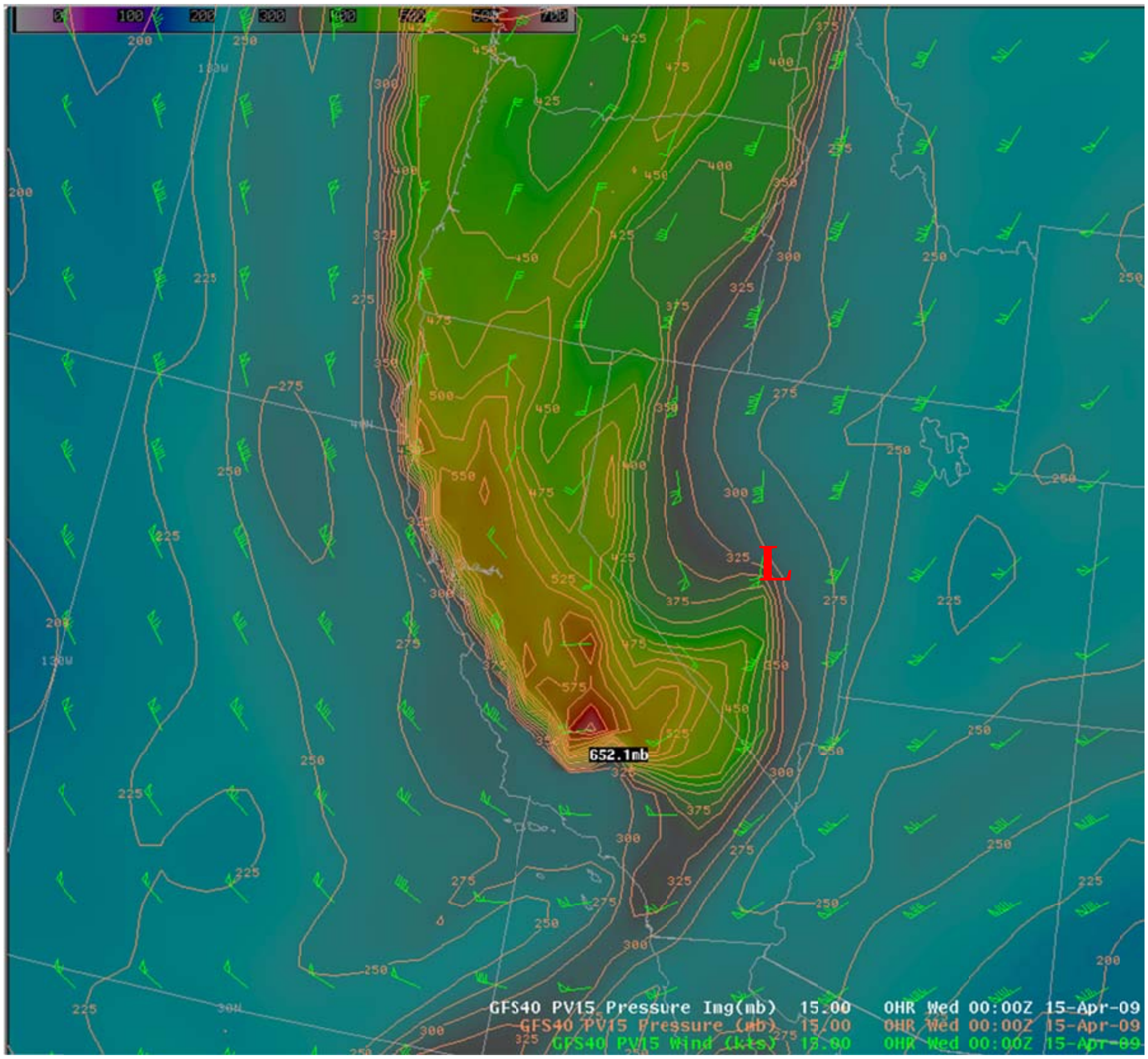


**Figure 10: GFS40 00-hour forecast depicting the pressure, in hPa, on the potential vorticity 1.5 surface (image and orange lines, solid) for 0000 UTC 15 April. The red "L" denotes the position of the surface low pressure system at this time.**

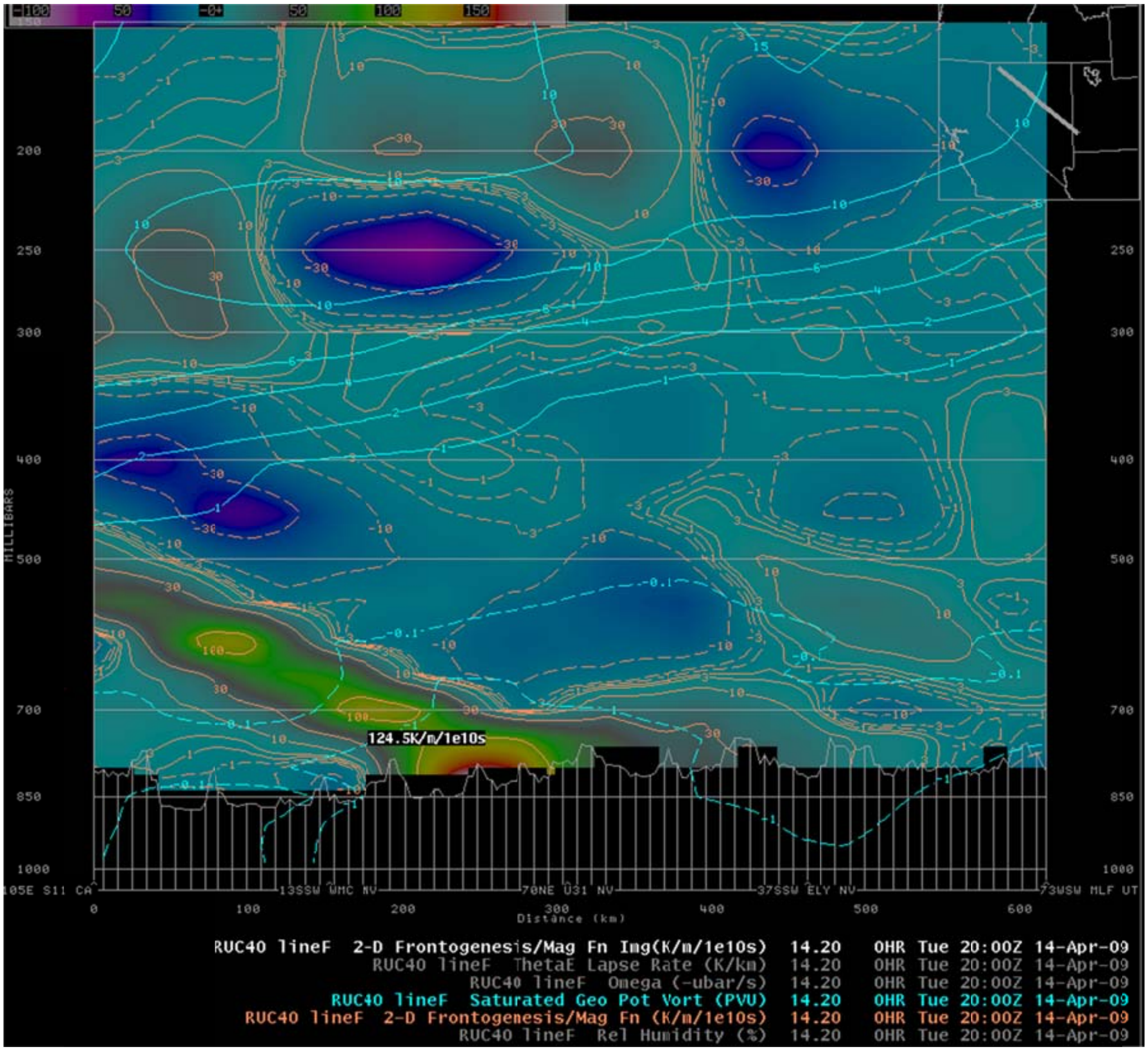


**Figure 11: RUC40 00-hour analysis depicting cross section of Petterssen Frontogenesis (image, orange lines) with saturated equivalent potential vorticity (cyan lines, dashed lines are negative) for 2000 UTC 14 April. The area of maximum frontogenesis begins roughly 70 NM NE of Austin, NV (KU31) shifting west-northwest to 13 NM south-southwest of Winnemucca, NV (KWMC). The cross section extends from near Pioche, NV in the southeast to near Denio, NV in the northwest (see inset, upper right).**

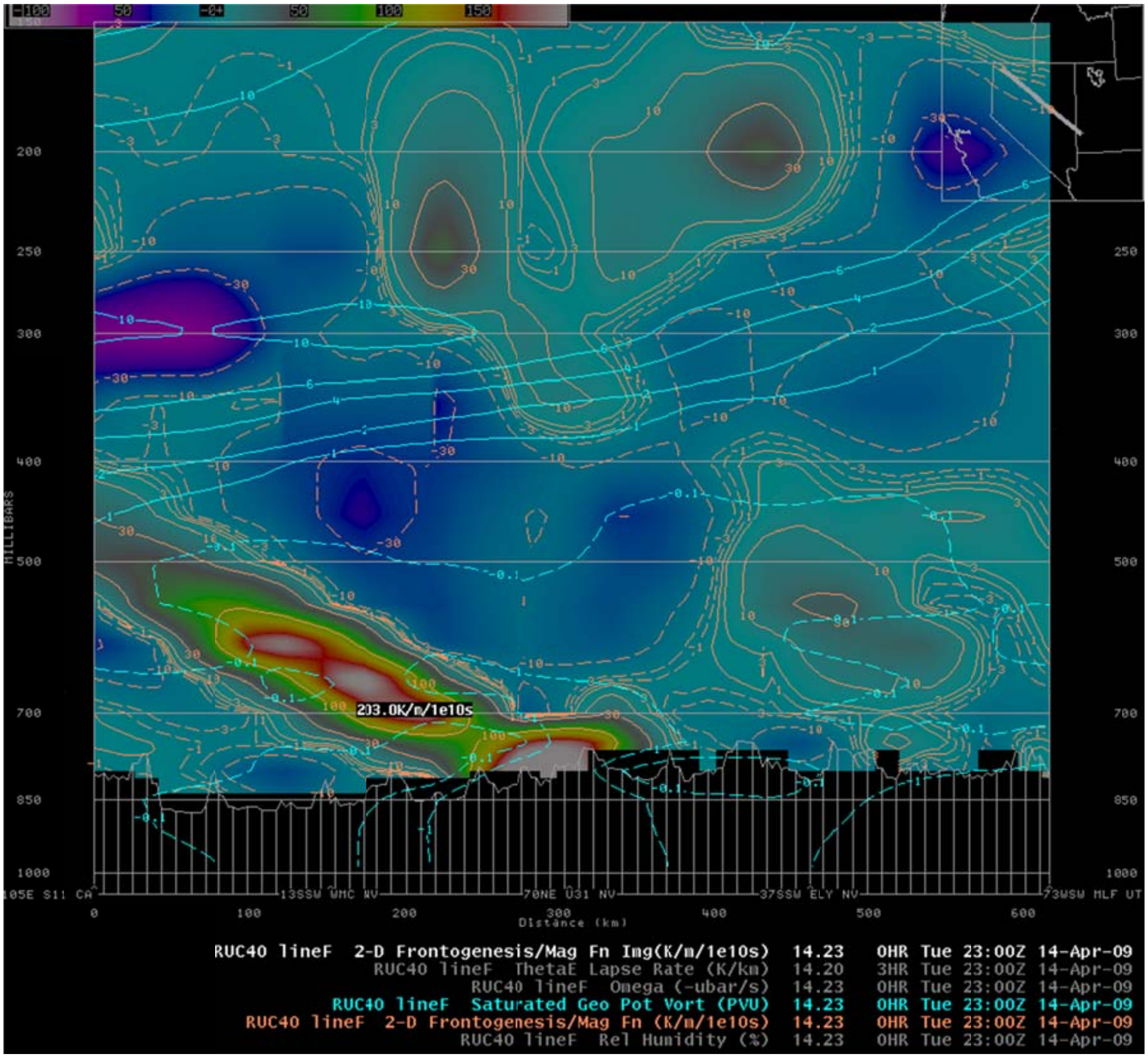


**Figure 12: Same as Figure 11 except time is 2300 UTC. Note the frontogenetic forcing increased significantly in a three hour period.**

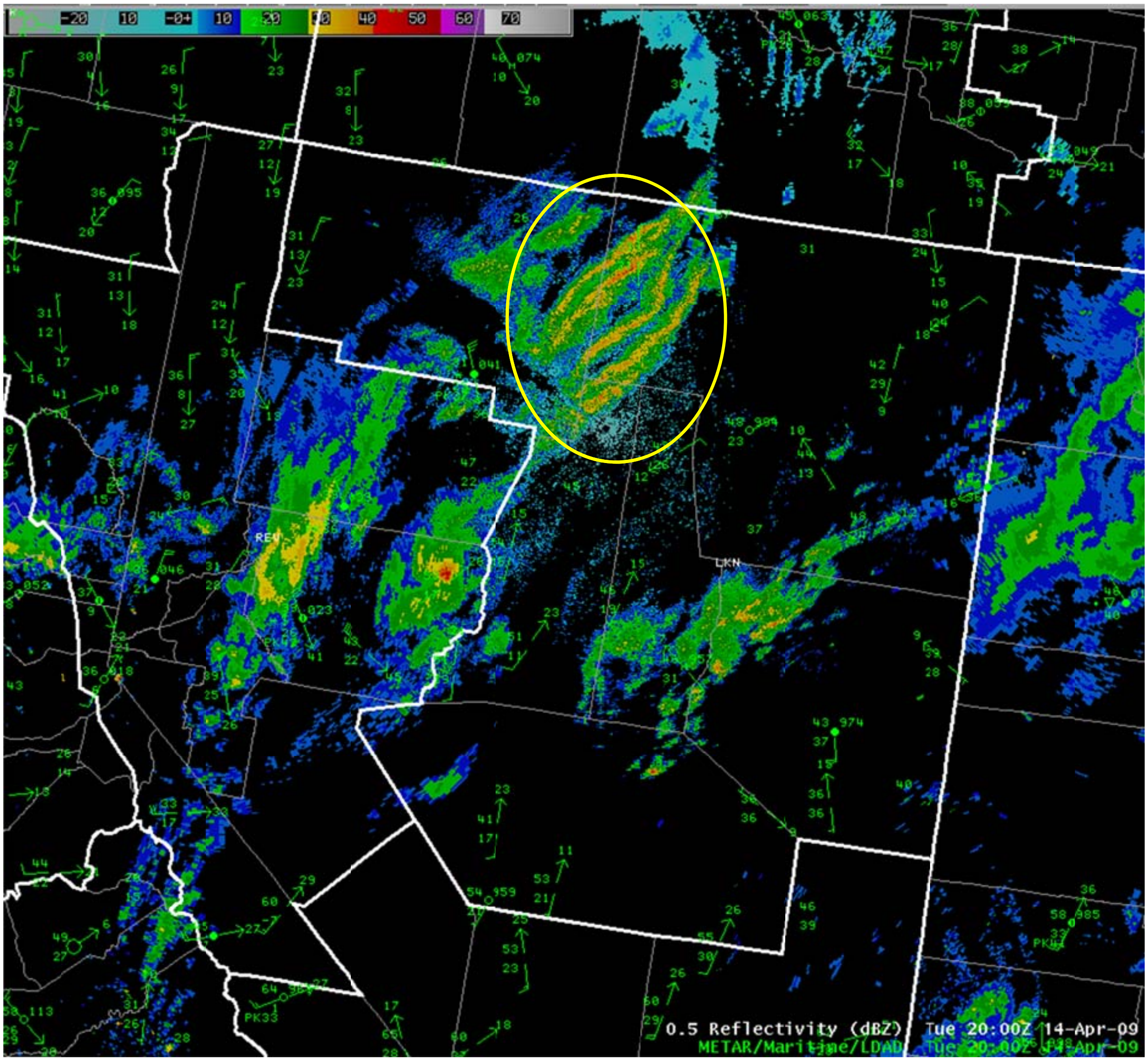


**Figure 13: Composite radar (reflectivity) shows developing showers in east-central Nevada, 2000 UTC on 14 April. The banding seen in northern Nevada (yellow circle) was caused by chaff released from military aircraft.**

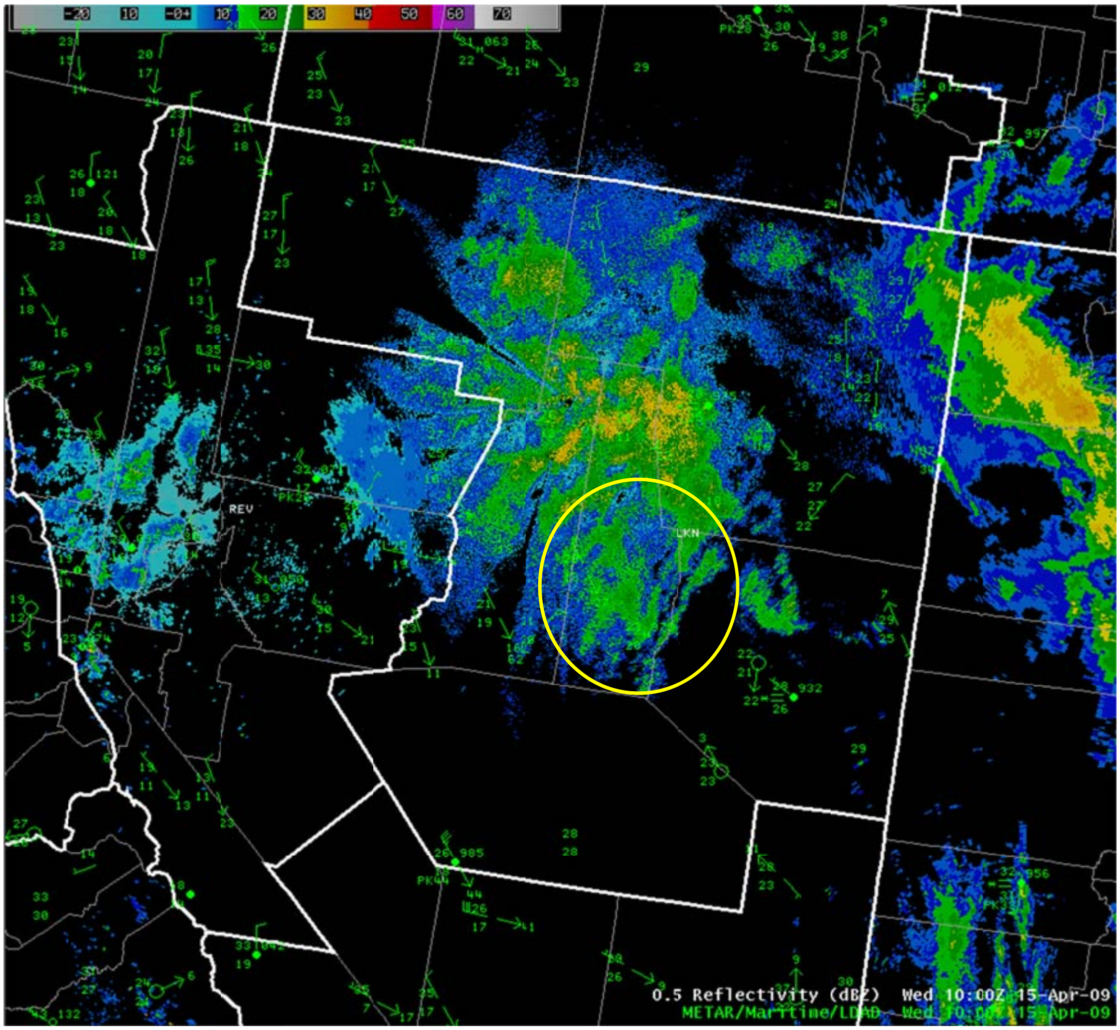

**Figure 14: Same as Figure 14 except time is 1000 UTC on 15 April. Shown in the yellow circle is evidence of banding in the precipitation shield.**

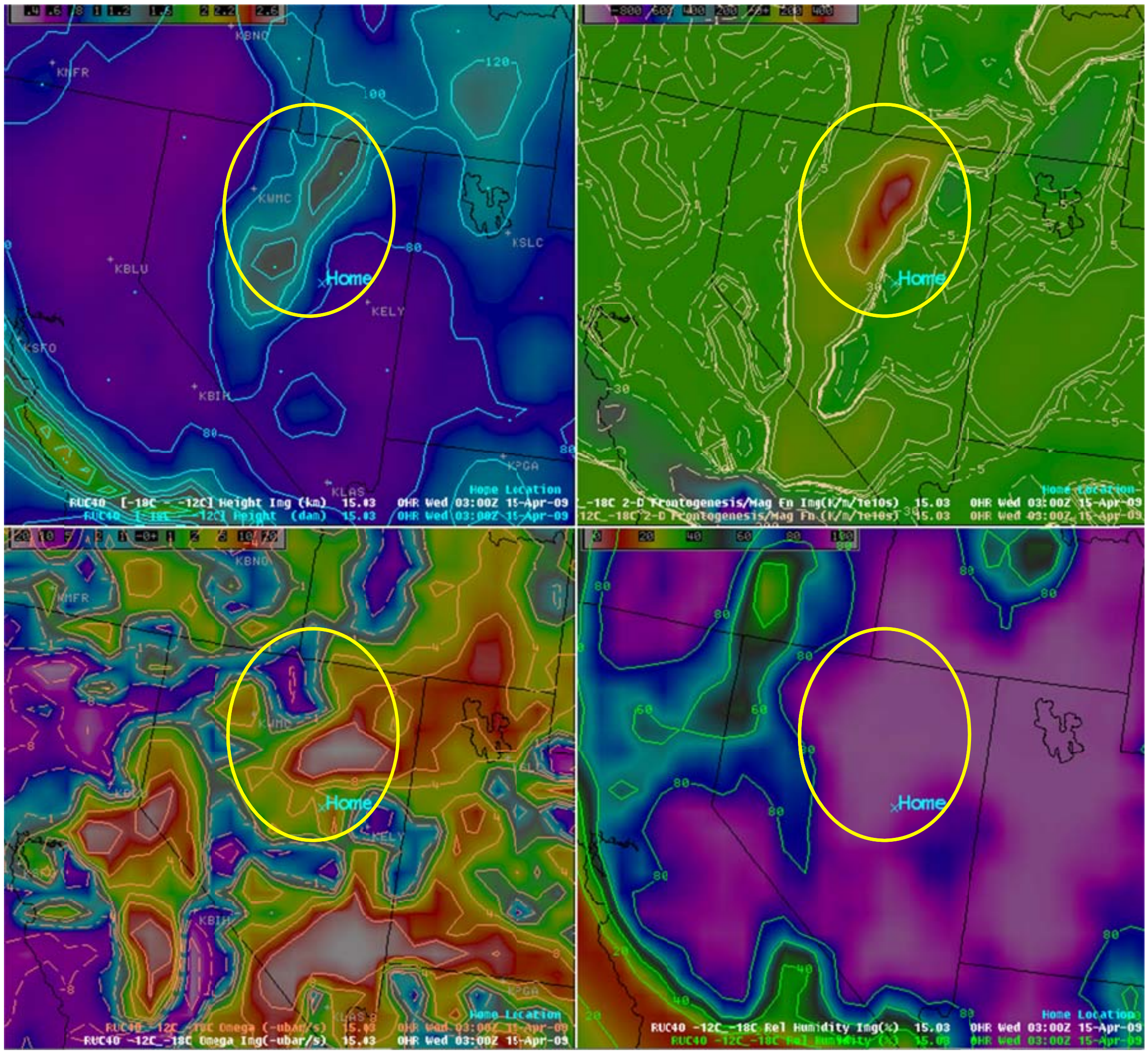


**Figure 15: RUC40 analysis 4-panel highlighting the -18 to -12C layer. Upper left shows the depth (km) of this layer (warm colors imply greater thicknesses), upper right shows frontogenesis (warmer colors imply greater frontogenesis forcing), lower right shows mean relative humidity (cool colors represent higher moisture levels), and lower left is layer mean omega (warmer colors indicate lift). 4-panel is for 0300 UTC 15 April. "Home" location is Eureka, Nevada (KP68). The yellow circles in the 4-panels depict a very thick -18C to -12C layer (upper left), corresponding strong frontogenesis in this same layer (upper right), with high omega values (lower left) and deep moisture (lower right).**

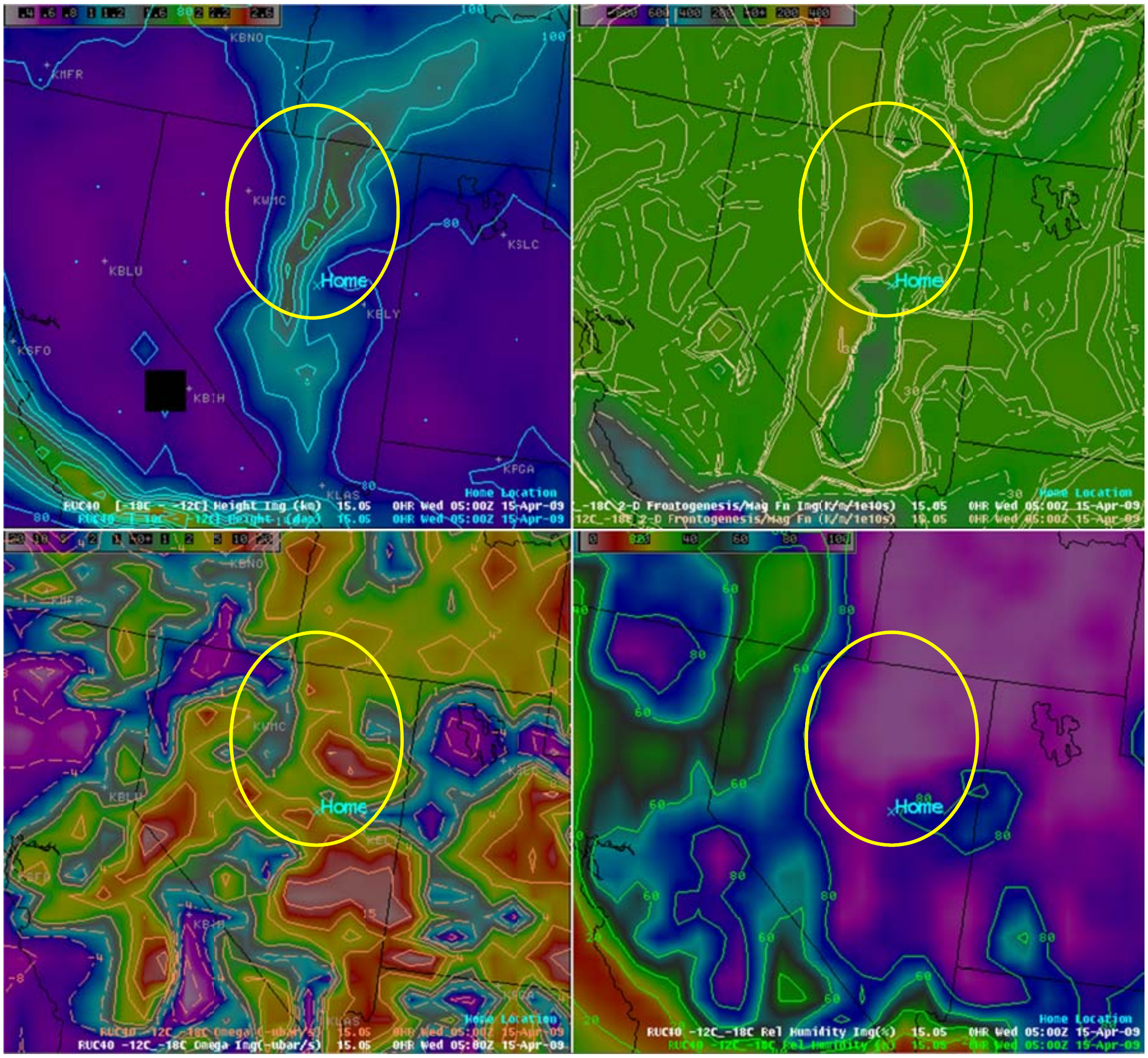


**Figure 16: Same as in Figure 15 except time is 0500 UTC 15 April.**

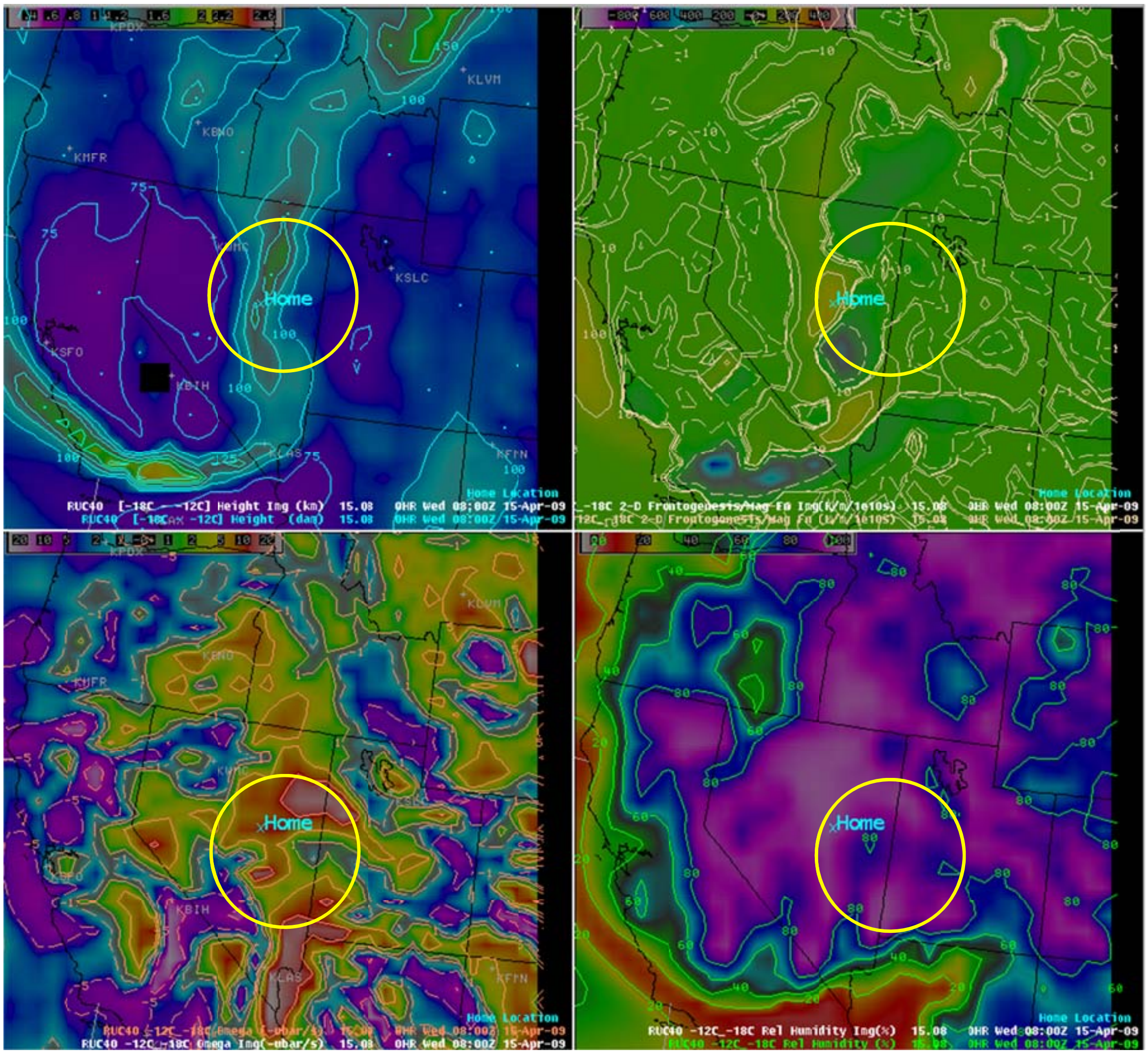

**Figure 17: Same as in Figure 15 except time is 0800 UTC 15 April.**

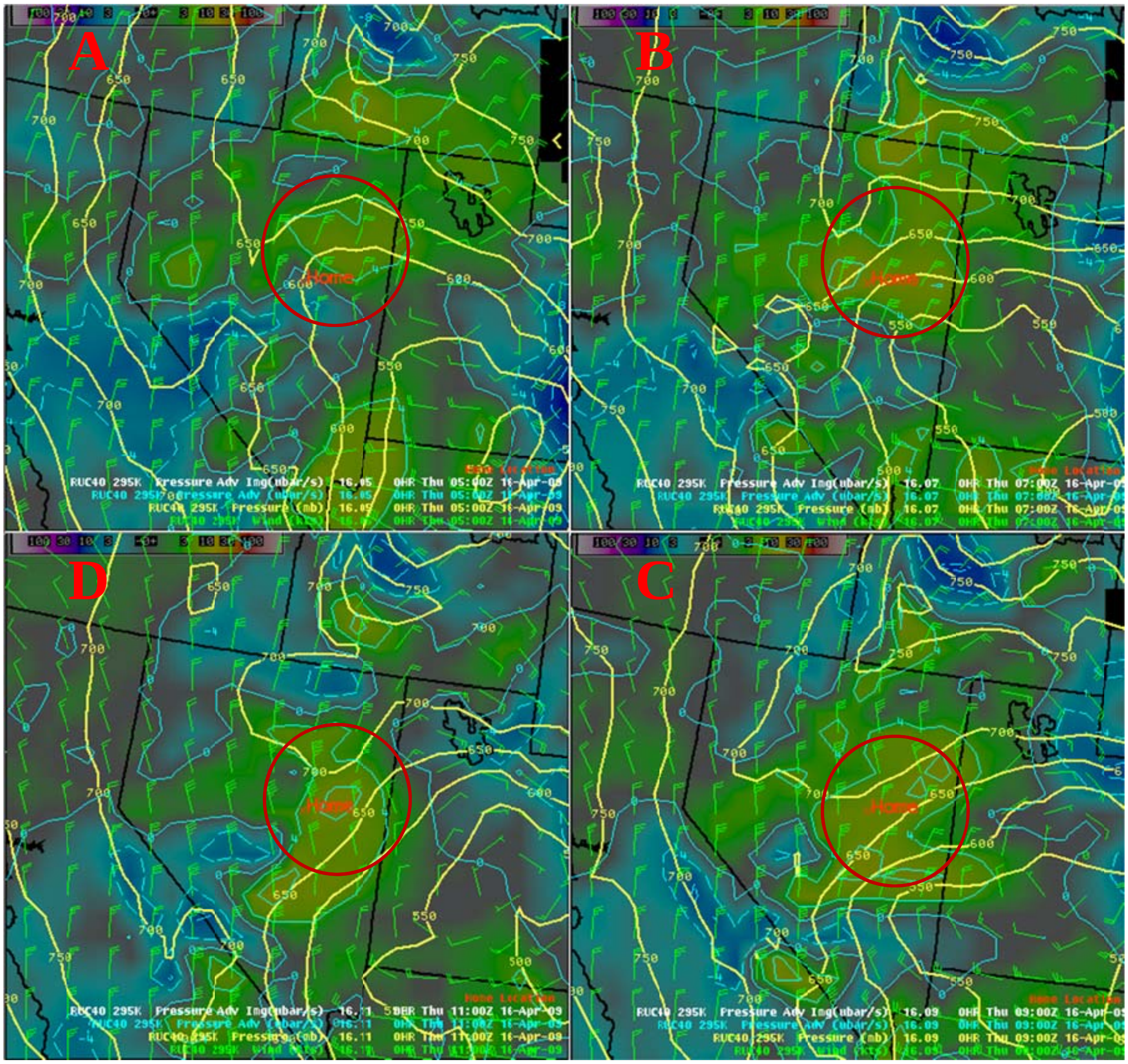


**Figure 18: RUC40 analysis of the 295K isentropic surface in 2-hour increments from 0500 UTC (A ), 0700 UTC (B), 0900 UTC (C) and 1100 UTC (D) on 16 April. Pressure in hPa is highlighted in yellow, bold solid lines. Wind is depicted in wind barbs (green). Pressure advection magnitude (thin blue lines, dashed lines are negative) with image (warmer colors represent positive values). "Home" position in red, denotes Eureka, Nevada (KP68). Red circles highlight high values of positive pressure advection (lift), as described in the text.**

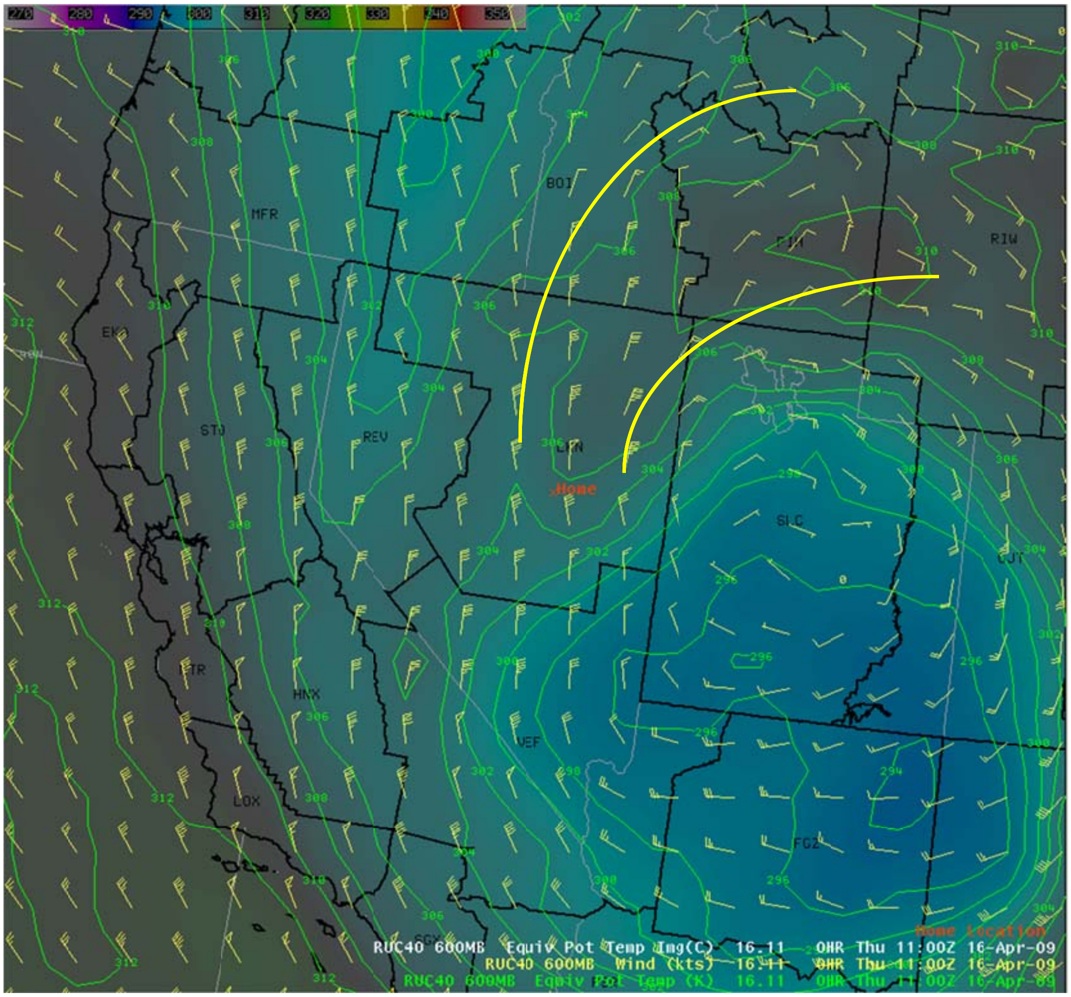


**Figure 19: RUC40 analysis depicting 600 hPa equivalent potential temperature (green lines, solid) for 1100 UTC 16 April. Warmer colors indicate higher moisture values. "Home" position in red is positioned over Eureka, Nevada (KP68). Golden arcs depict the area of maximum equivalent potential temperature (trowel-like feature).**

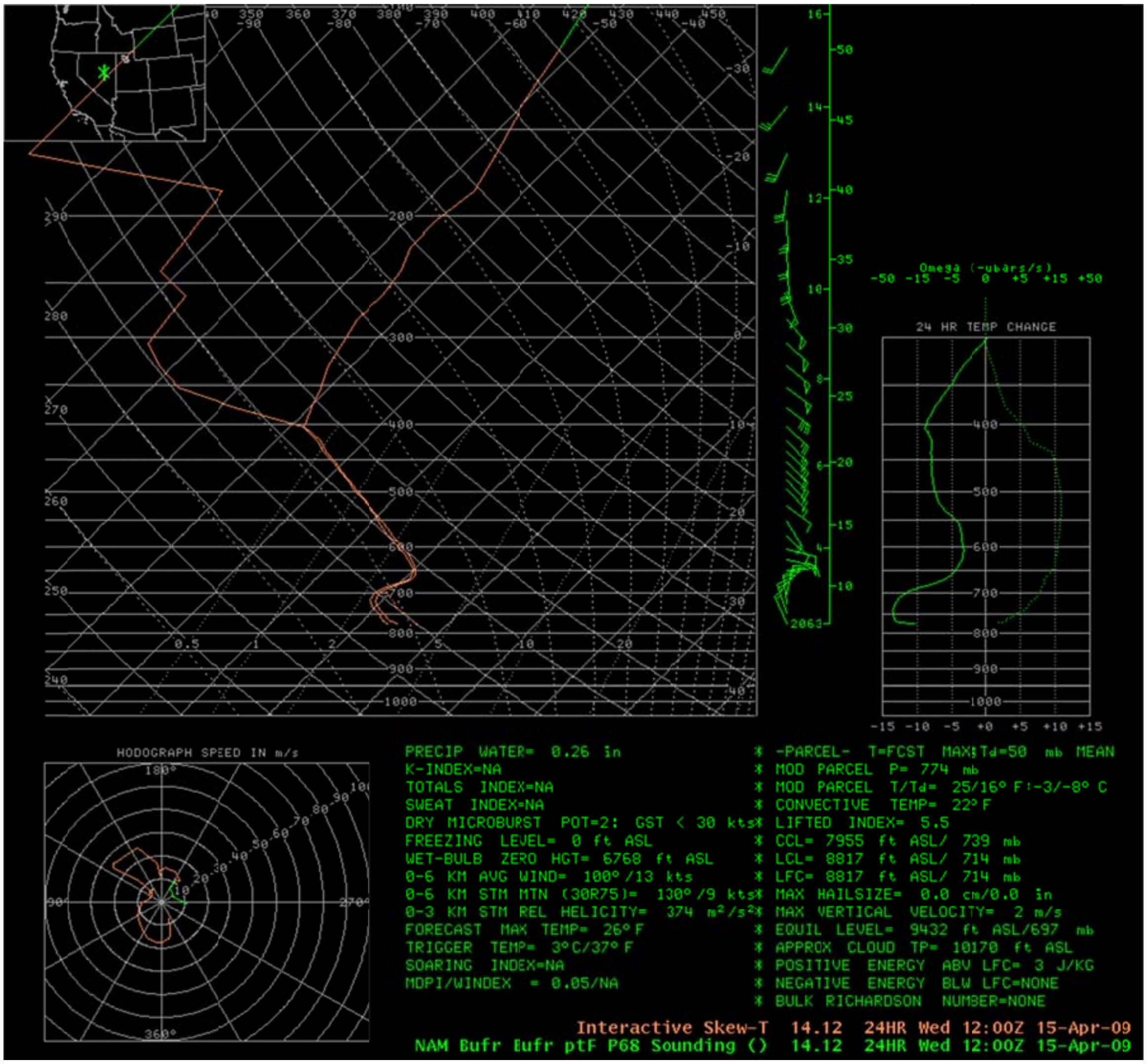

**Figure 20: NAM BUFR 12-hour forecast sounding for Eureka (KP68), NV at 1200 UTC 15 April.**


**Figure 21: MODIS image taken 17 Apr 2009 showing snow cover before and after the large snow storm. Stars indicate the locations of Lamoille, NV (north) and Eureka, NV (south) and arrows indicate the general low level wind direction for most of the event.**

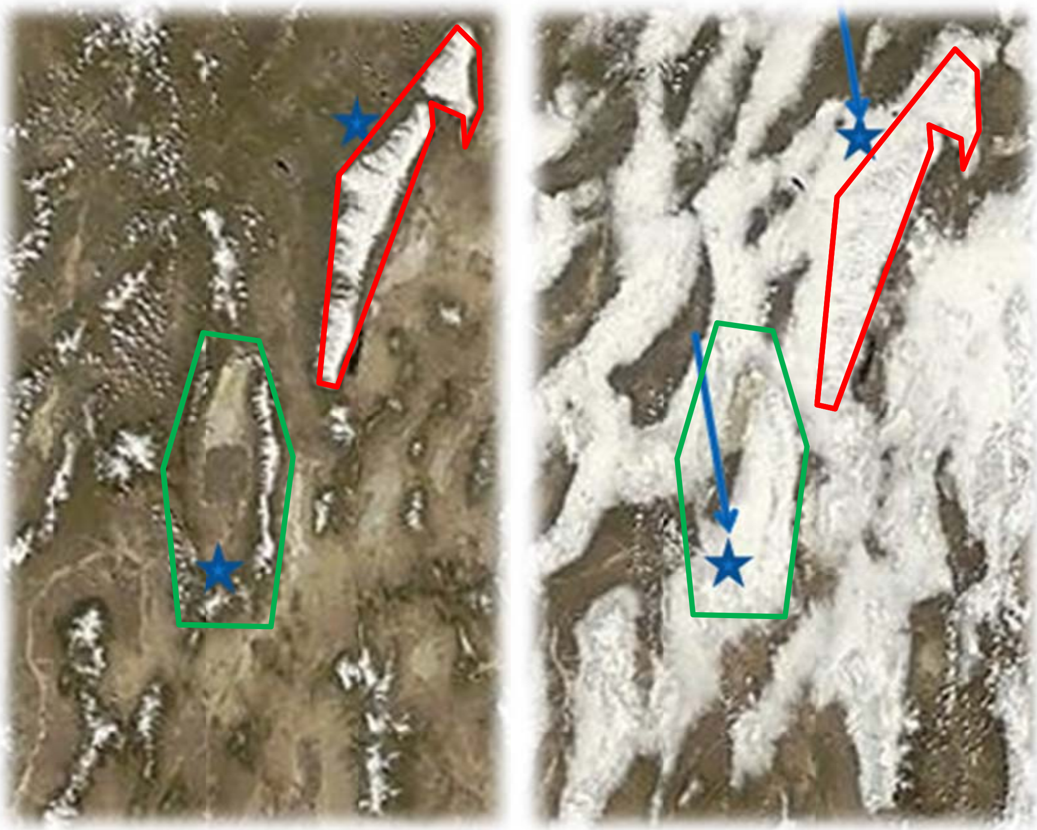

**Figure 22: MODIS imagery from Fig. 21 before (left) and after (right) the event, focusing on the Eureka and Lamoille areas. The green polygon shows the Diamond Valley area, while the red polygon shows the Ruby Mountains/East Humboldt Range. The favoring of the northwest slopes is evident in the image on the right, after the event.**